

**JAERI-Research**  
**95-062**



**PRESSURE DROP CHARACTERISTIC  
IN A CABLE-IN-CONDUIT CONDUCTOR**

**September 1995**

**Norikiyo KOIZUMI, Yoshikazu TAKAHASHI, Makoto SUGIMOTO  
Kazuya HAMADA, Takashi KATO, Hiroshi TSUJI  
and Susumu SHIMAMOTO**

**日本原子力研究所  
Japan Atomic Energy Research Institute**

本レポートは、日本原子力研究所が不定期に公刊している研究報告書です。

入手の問合わせは、日本原子力研究所技術情報部情報資料課（〒319-11 茨城県那珂郡東海村）あて、お申し越しください。なお、このほかに財団法人原子力弘済会資料センター（〒319-11 茨城県那珂郡東海村日本原子力研究所内）で複写による実費頒布をおこなっております。

This report is issued irregularly.

Inquiries about availability of the reports should be addressed to Information Division, Department of Technical Information, Japan Atomic Energy Research Institute, Tokai-mura, Naka-gun, Ibaraki-ken 319-11, Japan.

© Japan Atomic Energy Research Institute, 1995

---

編集兼発行	日本原子力研究所
印刷	いばらき印刷(株)

## Pressure Drop Characteristic in a Cable-in-conduit Conductor

Norikiyo KOIZUMI, Yoshikazu TAKAHASHI, Makoto SUGIMOTO, Kazuya HAMADA  
Takashi KATO, Hiroshi TSUJI and Susumu SHIMAMOTO

Department of Fusion Engineering Research  
Naka Fusion Research Establishment  
Japan Atomic Energy Research Institute  
Naka-machi, Naka-gun, Ibaraki-ken

(Received August 23, 1995)

A cable-in-conduit conductor (CICC) is the best candidate to satisfy requirement for a superconducting magnet to be employed in a fusion machine, such as a large operating current, high magnetic field, high breakdown voltage and so on. The pressure drop of the conductor is a key factor in design of a cryogenic pump to be used in a magnet system in the fusion machine. Also, pressure rise at a coil quench depends on the pressure drop characteristic of the conductor. Several workers investigated the pressure drop characteristic of CICCs. Katheder attempted to derive general correlation of the pressure drop characteristic basis on the correlation used for pebble beds. He compared his correlation with the measurements for the eight different CICCs. However, there is a large error of 75% in the maximum. It seems general formula of the pressure drop characteristic of CICC has not been provided. The authors investigate the pressure drop characteristic of 30 kA, 80 m cooling path length CICCs, whose dimension is almost same as the conductor to be employed in the fusion machine. The result indicates correlation between the Reynolds number and the friction factor of CICCs obeys the conventional formula for a smooth tube, Hagen-Poiseuille formula, in laminar flow region but does not agree with the conventional formula for a smooth tube, Blasius formula, in turbulent flow region. The experimental result is compared with Katheder's correlation. Katheder's correlation does not show good agreement with the experimental result in the turbulent flow region. The correlation that the friction factor is inversely proportional to 0.157 power of the Reynolds number and the proportional constant is

0.257 coincides better with the experimental result in this region.

Keywords: Superconducting, Pressure Drop, Cable-in-conduit

ケーブル・イン・コンジット導体の圧損特性

日本原子力研究所那珂研究所核融合工学部

小泉 徳潔・高橋 良和・杉本 誠・濱田 一弥  
加藤 崇・辻 博史・島本 進

(1995年8月23日受理)

核融合炉超電導コイルでは、大電流、高磁場、および高い絶縁性能等が要求される。ケーブル・イン・コンジット導体（C I C導体）は、これらの要求を満足できる導体として最有力視されている。C I C導体の圧損特性は、核融合炉用マグネットシステムで使用される循環ポンプの設計上重要である。また、コイル・クエンチ時の圧力上昇も導体の圧損特性によって決定される。C I C導体の圧損特性の研究は多数行われている。Kathederは石層の圧損式を基にC I C導体の圧損の一般式を導くことを試み、8つの実験結果と本式を比較した。実験結果と本式の間には、最大75%の誤差があり、C I C導体の圧損特性を与える一般式は確立されていない。そこで、核融合炉で実際に使用される規模の30kA級、80m冷却長C I C導体に対して、圧損特性の測定を行った。実験結果は、層流域ではC I C導体の圧損特性は、滑らかな円管の圧損特性を示すハーゲン・ポアズイユの法則に従うが、乱流域では、滑らかな円管の圧損特性を示すブラシウスの法則に従わないことが示された。Kathederの式と実験結果の比較も行った。Kathederの関係式は、乱流域では実験結果とあまりよく一致しなかった。乱流域では、圧損係数がレイノルズ数の0.157乗に反比例し、比例定数が0.257とした方が良い近似を与えられた。

## Contents

1. Introduction .....	1
2. Experiment .....	2
2.1 Main Parameters of the Conductor .....	2
2.2 Measurement .....	2
2.3 Experimental Result .....	5
3. Consideration .....	6
3.1 Comparison with Katheder's Correlation .....	6
3.2 New Correlation .....	7
4. Conclusion .....	8
Acknowledgement .....	9
Reference .....	10

## 目        次

1. 序 論 .....	1
2. 実 験 .....	2
2.1 導体諸元 .....	2
2.2 測定方法 .....	2
2.3 実験結果 .....	5
3. 考 察 .....	6
3.1 Kathederの関係式との比較 .....	6
3.2 新関係式 .....	7
4. 結 論 .....	8
謝 辞 .....	9
参考文献 .....	10

## Nomenclature

$L$ [m]	Cooling path length	$A_{He}$ [m <sup>2</sup> ]	Coolant cross sectional area
$Pe$ [m]	Wetted perimeter	$Pe_{con}$ [m]	Conduit wetted perimeter
$D_h$ [m]	Hydraulic diameter	$d$ [m]	Strand diameter
$\nu$	Void fraction	$\rho$ [kg/m <sup>3</sup> ]	Coolant density
$\dot{m}$ [kg/sm <sup>2</sup> ]	Coolant mass flow flux	$\dot{M}$ [kg/s]	Coolant mass flow rate
$\mu$ [kg/ms]	Coolant viscosity	$Re$	Reynolds number
$Re_c$	Critical Reynolds number	$f$	Friction factor
$f_l$	Friction factor in laminar flow region		
$f_t$	Friction factor in turbulent flow region		
$\Delta P$ [Pa]	Pressure drop of unit cooling path length		

# 1 Introduction

A cable-in-conduit conductor (CICC) is the best candidate for application of a superconductor to large and high magnetic field coils in a tokamak fusion reactor since it can provide high-voltage integrity, robust structure and so on. In particular, its low AC loss characteristic is excellent in the application to a Poloidal field coil. Applicability of CICC to a fusion machine were demonstrated through the Demo Poloidal Coil (DPC) experiments<sup>1-4</sup>. Also, CICC will be employed in the next fusion machine, International Thermonuclear Experimental Reactor (ITER)<sup>5</sup>.

Superconducting strands in CICC are cooled by supercritical helium (SHe) flowing in the conductor. SHe usually flows a closed circuit consisting of coils, cryogenic circulation pumps, heat exchangers and so on in a large magnet system. The pressure drop characteristic of the conductor is of importance in design of the cryogenic circulation pump.

Also, pressure rise during a coil quench depends on the pressure drop characteristic of the conductor since large induced flow is generated in the conductor at that time. Rapid pressure rise may cause damage of the conductor and/or insulation of the conductor. Evaluation of the pressure rise at a coil quench is then one of the most important works in conductor design. For this evaluation, the pressure drop characteristic should be clarified.

Several workers investigated the pressure drop characteristic of CICC<sup>6-12</sup>. Katheder<sup>10,11</sup> attempted to derive a general correlation between the Reynolds number and the friction factor basis on the correlation used for pebble beds. He compared his correlation with the measurements for the eight different CICC. However, there is a large error of 75% in the maximum<sup>10,11</sup>. It seems the general formula of the pressure drop characteristic of CICC has not been established. The pressure drop characteristic of DPC-U1 and DPC-U2<sup>13,14</sup> conductors whose dimension and length are almost same as the one to be employed in a fusion machine was investigated during and after cooldown of the coils to evaluate the pressure drop characteristic of the conductors for the fusion machine. Hereafter, DPC-U1 and -U2 are collectively called as 'DPC-U'. The experimental results are reported in this paper.

In addition, the experimental result is compared with the correlation derived by

Katheder.

## 2 Experiment

### 2.1 Main parameters of the conductor

The cable of the DPC-U conductor consists of 486 twisted strands whose diameter is 1.12 mm and is jacketed by 2-mm thick stainless steel conduit. Void fraction of the DPC-U conductor is 38%. The cross section of the DPC-U conductor is shown in Fig. 1.

The conductor is wound into a double pancake with inner diameter of 1 m and outer diameter of 2 m. Each of DPC-U is composed of four double pancakes, each of which is termed as A- to H-pancake as shown in Fig. 2. The coolant flow from the innermost turn to the outermost turn. Unit length of the conductor is 160 m and then the cooling path length is 80 m. The main parameters of the conductors are listed in Table 1.

### 2.2 Measurement

The pressure drop characteristic is investigated in the A-pancake of DPC-U1 and -U2

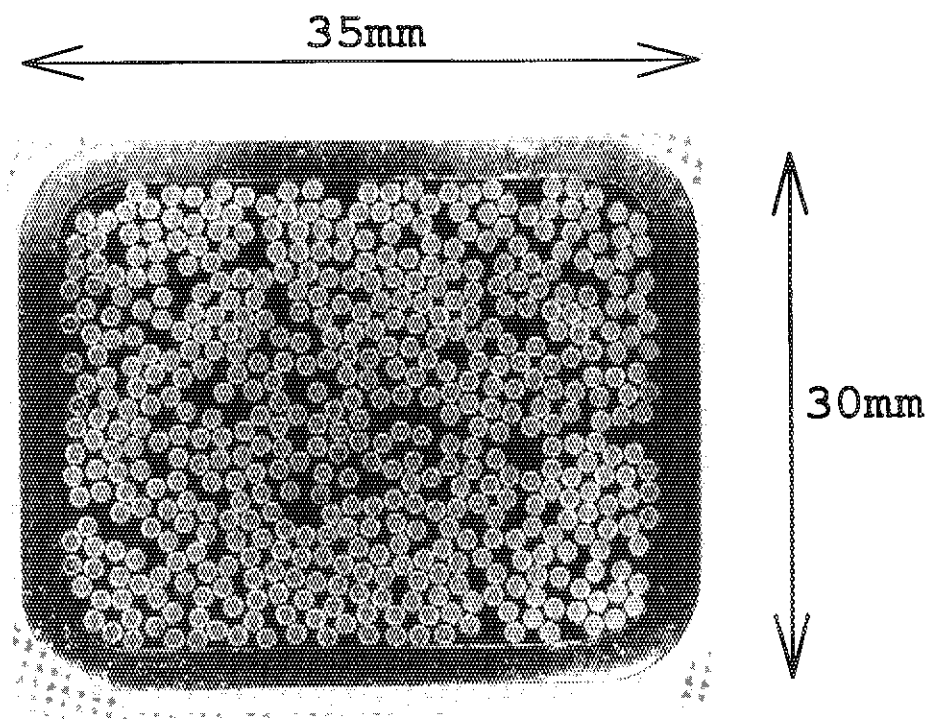


Fig. 1 Cross sectional view of the sample conductor

Katheder.

## 2 Experiment

### 2.1 Main parameters of the conductor

The cable of the DPC-U conductor consists of 486 twisted strands whose diameter is 1.12 mm and is jacketed by 2-mm thick stainless steel conduit. Void fraction of the DPC-U conductor is 38%. The cross section of the DPC-U conductor is shown in Fig. 1.

The conductor is wound into a double pancake with inner diameter of 1 m and outer diameter of 2 m. Each of DPC-U is composed of four double pancakes, each of which is termed as A- to H-pancake as shown in Fig. 2. The coolant flow from the innermost turn to the outermost turn. Unit length of the conductor is 160 m and then the cooling path length is 80 m. The main parameters of the conductors are listed in Table 1.

### 2.2 Measurement

The pressure drop characteristic is investigated in the A-pancake of DPC-U1 and -U2

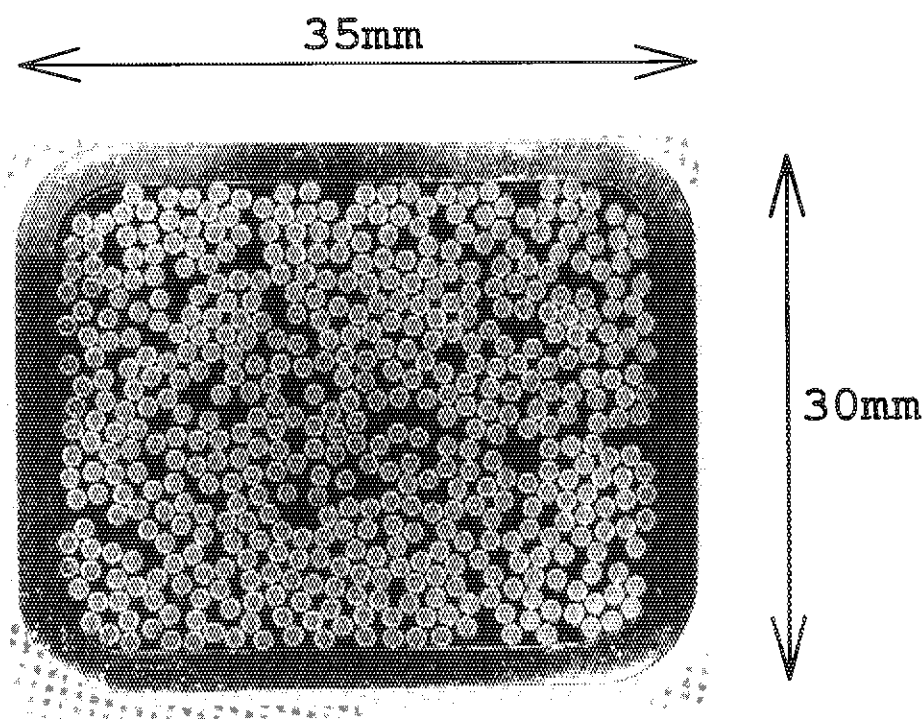


Fig. 1 Cross sectional view of the sample conductor

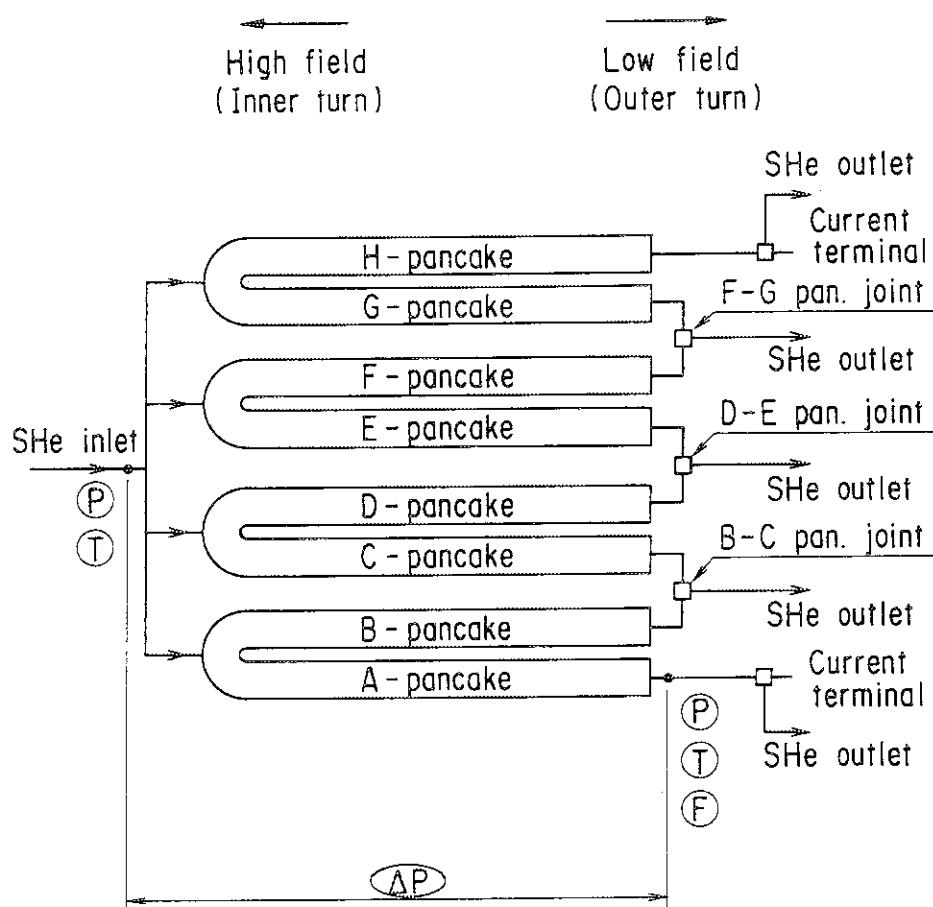


Fig. 2 Schematic configuration of DPC-U. T, P, F and  $\Delta P$  in the figure indicate the location where the coolant temperature, pressure, mass flow rate and pressure drop were measured.

during and after the cooldown in the latest DPC experiment<sup>4</sup>. Figure 3 shows a coil assembly of DPC-U1, -U2 and test coil, installed between DPC-U1 and -U2, in the DPC test facility<sup>15</sup>.

The friction factor and the Reynolds number are defined by the following equations.

$$f = \frac{D_h}{L} \frac{2\rho\Delta P}{\dot{m}^2} \quad (1)$$

$$Re = \frac{\dot{m}D_h}{\mu} \quad (2)$$

Where,

$$\dot{m} = \frac{\dot{M}}{A_{He}} \quad (3)$$

Table 1 Main parameters of the DPC-U conductor

Length of unit cooling channel	80 m
Inner winding diameter of pancake	1 m
Outer winding diameter of pancake	2 m
Conductor outside dimension	30 × 35 mm
Conductor inner dimension	26 × 31 mm
Number of strands	486
Twisting length	
First stage	90 mm
Second stage	180 mm
Third stage	240 mm
Forth stage	480 mm
Fifth stage	950 mm
Void fraction	38%
Hydraulic diameter	0.665 mm
Strand Diameter	1.12 mm

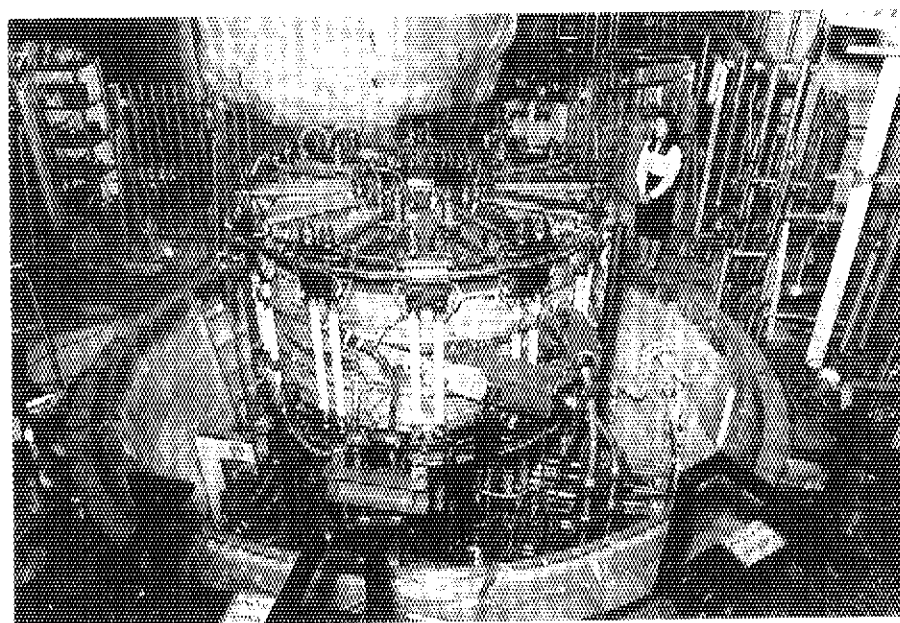


Fig. 3 Coil assembly of DPC-U1, -U2 and test coil in the DPC test facility.

The thermal properties of helium are calculated by employing a helium thermal property calculation library<sup>16</sup>. Hydraulic diameter is defined by,

$$D_h = \frac{4A_{He}}{Pe} \quad (4)$$

Circumference of the strands are usually multiplied by 5/6 in the estimation of the wetted perimeter as the follows since the circumference surrounded by triplex is believed to take no effect on the pressure drop.

$$Pe = 486\pi d \times \frac{5}{6} + Pe_{con} \quad (5)$$

However, this is true only when the coolant surrounded by the triplex is completely isolated from the coolant at the triplex outside. In the DPC-U conductor, we cannot recognize what three strands compose the triplex from the DPC-U conductor cross sectional view shown in Fig. 1. It is because of the long length twisting pitch and the high void fraction of the DPC-U conductor. Therefore, the circumference of the strands is not multiplied by 5/6 in the estimation of the wetted perimeter in the DPC-U conductor. The wetted perimeter is then calculated from,

$$Pe = 486\pi d + Pe_{con} \quad (6)$$

Note that the circumference of the stainless steel tape, wrapping the cable, is neglected since there exists almost no space between the tape and the inner surface of the conduit as shown in Fig. 1.

Temperature and pressure of the coolant were measured at the inlet and the outlet of the coolant. Their averages are used for the calculation of the friction factor and the Reynolds number. The temperature difference between the inlet and the outlet was controlled so as to be less than 80 K during the cooldown. The data of the Reynolds number of less than about 2000 were acquired during the cooldown. The other data were acquired after the cooldown. After the cooldown, the temperature difference between the inlet and the outlet was less than 0.5 K.

## 2.3 Experimental result

Figure 4 shows the experimental results of the pressure drop characteristic of the DPC-U1 and -U2 conductors. The measured friction factor is dominated by the general

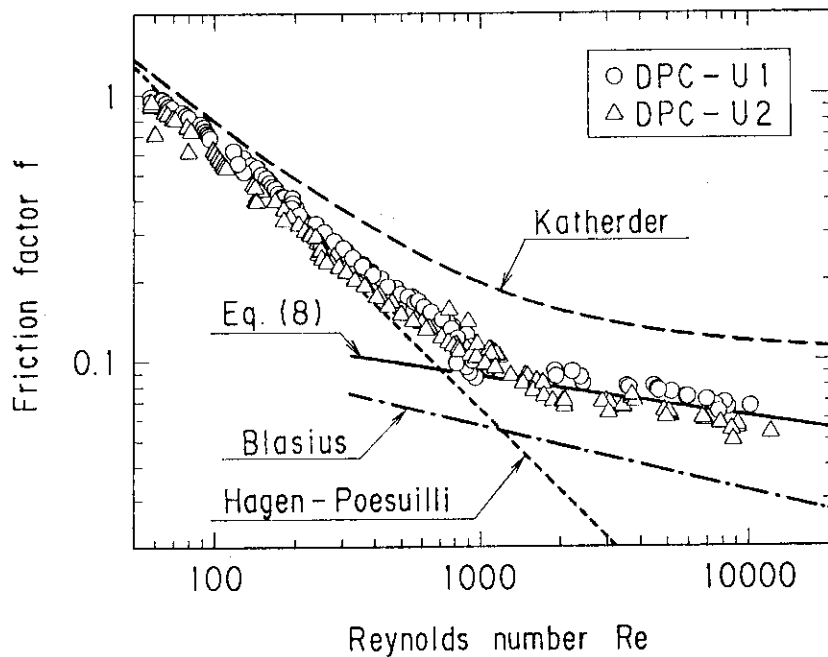


Fig. 4 Measured and calculated friction factor as a function of Reynolds number. The wetted perimeter is calculated by equation (6).

formula for laminar flow in a smooth tube, Hagen-Poesuilli formula, in the low Reynolds number region as shown in Fig. 4. However, in the high Reynolds number region, the measured friction factor is higher than that calculated for a smooth tube according to Blasius formula as shown in Fig. 4.

The transition from laminar flow to turbulent flow was not observed in this experiment as well as in the experiments by other workers<sup>6-12</sup>.

### 3 Consideration

#### 3.1 Comparison with Katheder's correlation

The experimental result is compared with the correlation derived by Katheder<sup>10,11</sup>. The Katheder's correlation<sup>10,11</sup> is,

$$f = \frac{1}{v^{0.72}} \left( \frac{19.5}{Re^{0.88}} + 0.051 \right) \quad (7)$$

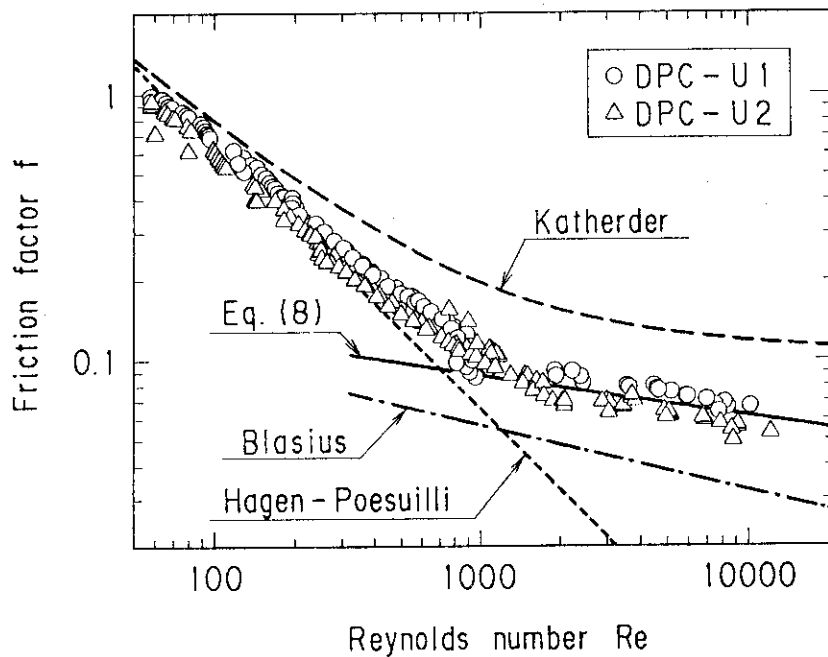


Fig. 4 Measured and calculated friction factor as a function of Reynolds number. The wetted perimeter is calculated by equation (6).

formula for laminar flow in a smooth tube, Hagen-Poesuilli formula, in the low Reynolds number region as shown in Fig. 4. However, in the high Reynolds number region, the measured friction factor is higher than that calculated for a smooth tube according to Blasius formula as shown in Fig. 4.

The transition from laminar flow to turbulent flow was not observed in this experiment as well as in the experiments by other workers<sup>6-12</sup>.

### 3 Consideration

#### 3.1 Comparison with Katheder's correlation

The experimental result is compared with the correlation derived by Katheder<sup>10,11</sup>. The Katheder's correlation<sup>10,11</sup> is,

$$f = \frac{1}{v^{0.72}} \left( \frac{19.5}{Re^{0.88}} + 0.051 \right) \quad (7)$$

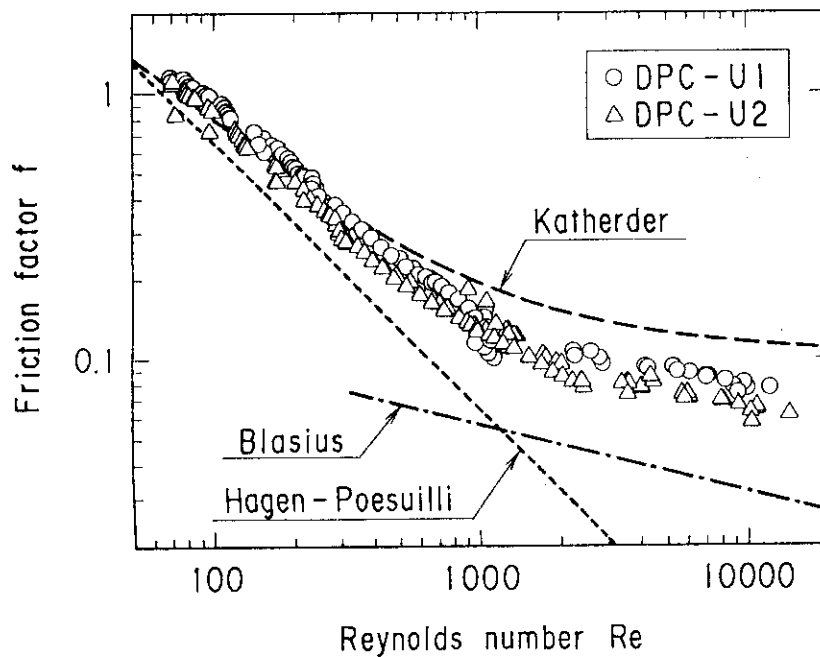


Fig. 5 Measured and calculated friction factor as a function of Reynolds number. The wetted perimeter is calculated by equation (5).

In Fig. 4, the Katheder's correlation is shown for comparison. This correlation disagrees with the experimental results in the high Reynolds number region.

The wetted perimeter is defined by equation (5) in Katheder's correlation. Figure 5 shows the experimental results when the wetted perimeter is calculated by equation (5) and Katheder's correlation. The agreement between the Katheder's correlation and the experimental result is improved by using equation (5). However, there still exists large error between them in the high Reynolds number region.

### 3.2 New correlation

The flow of the coolant in the conductor is generally in the turbulent flow region to obtain high heat transfer performance. The disagreement in the turbulent flow region is not therefore acceptable. New correlation showing good agreement in the turbulent flow region is then provided. From the experimental result, the friction factor in the turbulent flow region can be approximated by,

$$f_t = \frac{0.257}{Re^{0.157}} \quad (8)$$

The correlation calculated by equation (8) is shown in Fig. 4.

For the estimation of the pressure rise during a coil quench, it should be possible to calculate the friction factor on the low Reynolds number region. The experimental result indicates Hagen-Poesuilli formula gives good approximation in the low Reynolds number region. Consequently, the friction factor is approximated by the following equation with equation (8),

$$f = \begin{cases} f_l & (Re \leq Re_c) \\ f_t & (Re_c < Re) \end{cases} \quad (9)$$

Where,

$$f_l = \frac{64}{Re} \quad (\text{Hagen-Poesuilli}) \quad (10)$$

The transition from the laminar to turbulent flow was not observed in the experiment. Therefore, we cannot define the critical Reynolds number. The critical Reynolds number is however defined as the one at the intersection of the curves calculated by equations (8) and (10), for convenience. The value of this pseudo critical Reynolds number is about 700.

## 4 Conclusion

The pressure drop characteristic was investigated. The conductors are 30 kA, 80 m cooling path length CICC's whose dimension is almost same as the conductor to be employed in the fusion machine. The friction factor was measured as a function of the Reynolds number during and after the cooldown of the coils. The range of the Reynolds number was  $50 < Re < 20000$ . The experimental results are:

- 1) In the low Reynolds number region, the relation between the friction factor and the Reynolds number is in accordance with the conventional formula for laminar flow, Hagen-Poesuilli formula.
- 2) The transition from laminar flow to turbulent flow was not observed.
- 3) The correlation derived by Katheder cannot show good agreement with our experimental result in high Reynolds number region. In this region, the friction factor

$$f_t = \frac{0.257}{Re^{0.157}} \quad (8)$$

The correlation calculated by equation (8) is shown in Fig. 4.

For the estimation of the pressure rise during a coil quench, it should be possible to calculate the friction factor on the low Reynolds number region. The experimental result indicates Hagen-Poesuilli formula gives good approximation in the low Reynolds number region. Consequently, the friction factor is approximated by the following equation with equation (8),

$$f = \begin{cases} f_l & (Re \leq Re_c) \\ f_t & (Re_c < Re) \end{cases} \quad (9)$$

Where,

$$f_l = \frac{64}{Re} \quad (\text{Hagen-Poesuilli}) \quad (10)$$

The transition from the laminar to turbulent flow was not observed in the experiment. Therefore, we cannot define the critical Reynolds number. The critical Reynolds number is however defined as the one at the intersection of the curves calculated by equations (8) and (10), for convenience. The value of this pseudo critical Reynolds number is about 700.

## 4 Conclusion

The pressure drop characteristic was investigated. The conductors are 30 kA, 80 m cooling path length CICC's whose dimension is almost same as the conductor to be employed in the fusion machine. The friction factor was measured as a function of the Reynolds number during and after the cooldown of the coils. The range of the Reynolds number was  $50 < Re < 20000$ . The experimental results are:

- 1) In the low Reynolds number region, the relation between the friction factor and the Reynolds number is in accordance with the conventional formula for laminar flow, Hagen-Poesuilli formula.
- 2) The transition from laminar flow to turbulent flow was not observed.
- 3) The correlation derived by Katheder cannot show good agreement with our experimental result in high Reynolds number region. In this region, the friction factor

is inversely proportional to 0.157 power of Reynolds number and the proportional constant is 0.257.

## Acknowledgment

The authors would like to thank Drs. Y. Tanaka, M. Ohta and T. Nagashima for their encouragement and support during this work. Authors would also like to thank to all staff members of the Superconducting Magnet Laboratory in Japan Atomic Energy Research Institute. Mitsubishi Electric Co. Ltd, Showa Electric Wire & Cable Co. Ltd and Fuji Electric Co. Ltd are gratefully acknowledged for their manufacturing contributions.

is inversely proportional to 0.157 power of Reynolds number and the proportional constant is 0.257.

## Acknowledgment

The authors would like to thank Drs. Y. Tanaka, M. Ohta and T. Nagashima for their encouragement and support during this work. Authors would also like to thank to all staff members of the Superconducting Magnet Laboratory in Japan Atomic Energy Research Institute. Mitsubishi Electric Co. Ltd, Showa Electric Wire & Cable Co. Ltd and Fuji Electric Co. Ltd are gratefully acknowledged for their manufacturing contributions.

## Reference

- 1 Takahashi, Y., Yoshida, K., Ando, T. and Tsuji, H., *et al. Cryogenics* (1991) **31** 640
- 2 Steeves, M., Takayasu, M., Painter, T., Hoenig, M., *et al. Adv. Cryog. Eng.* (1991) **37** 345
- 3 Nishi, M., Ando, T., Tsuji, H., Mukai, H., *et al. Cryogenics.* (1993) **33** 573
- 4 Ando, T., Nakajima, H., Sasaki, T., Hiyama, Y., *et al. Advances in Cryogenic Engineering* (1994) Vol. **39** 335
- 5 Thome, R. J. *IEEE Trans. on Magnet* (1994) **30** No.4 1595
- 6 Janocko, M., Blaughter, R. and Eckels, P. *ICEC* 7 (1978) 679
- 7 Lue, J., Miller, J. and Lottin, J. *IEEE Trans. on Magnet* **MAG-15** No.1 (1979) 53
- 8 Iida, F., Hotta, Y., Takahashi, R., Hara, N. *et al. ICEC* 12 (1988) 831
- 9 Tada, E., Takahashi, Y., Tsuji, H., Okuno, K. *et al. Cryogenics* (1991) **32** 829
- 10 Katheder, H. The NET team, Internal note N/R/0821/26/A
- 11 Katheder, H. *Cryogenics* (1994) **34** 595
- 12 Maekawa, R. Smith, M. and Van Sciver, S. *ASC* 1994
- 13 Koizumi, N., Okuno, K., Takahashi, Y., Tsuji, H., *et al. Cryogenics* (1994) **34** 155.
- 14 Koizumi, N., Okuno, K., Takahashi, Y., Tsuji, H., *et al. Cryogenics*, (1994) **34** 1015
- 15 Shimamoto, S., Okuno, K., Ando, T., Hiyama, T. *et al. Proc. MT-11* Elsevier Science Publisher, Essex, UK (1990) 23
- 16 Arp, V. and McCarty, R. *Thermophysical Properties of Helium-4 From 0.8 to 1500 K With Pressures to 2000 MPa*, NITS Tech Note 1334 US Government Printing Office, Washington, USA (1989)